

Prompt photon production in the k_T -factorization: parton Reggeization approach

M.A. Nefedov^{1,2}, A.V. Karpishkov^{1,3}, V.A. Saleev^{1,3}, and A.V. Shipilova^{1,3}

(1) Samara National Research University,

(2) Hamburg University,

(3) Joint Institute for Nuclear Research, Dubna

05.02.2020

Workshop on Correlations in Partonic and Hadronic Interactions (CPHI-2020)

Outline.

- 1 Introduction
- 2 Parton Reggeization Approach: k_T -factorization and Lipatov's effective action
- 3 Prompt photon production at high energy: single, associated, double (a review of calculations in the PRA)
- 4 KMR unPDFs ($x \ll 1$) and modified KMR unPDFs ($x < 1$).
- 5 Prompt photon production in the PRA at low energy (down to energies of SPD NICA and COMPASS++/AMBER)
- 6 Conclusions

Introduction

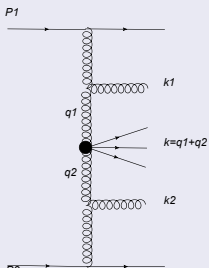
Prompt photon production as tool to explore the structure of hadrons, the spin content of the nucleons and to test perturbative QCD

Photons with large transverse momenta, p_T

- Prompt = Direct + Fragmentation Production
- Direct photons are produced in parton-parton interaction, $q + \bar{q} \rightarrow \gamma + g$,
 $q + g \rightarrow q + \gamma$
- Fragmentation production, $q + q \rightarrow q[\gamma] + q$. It can be suppressed by experimental conditions.
- Parton-to-photon Fragmentation Function (FF) can be calculated in QCD and FF is important ingredient of High Order calculations in QCD
- Large- p_T photon production has clean experimental signal and one was (is) studying at many accelerators at high energies.

Parton Reggeization Approach

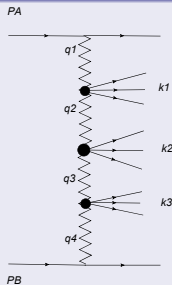
Schematic representation of the amplitude in CPM



$$k_{T1,2} \sim q_{T1,2} \sim 0$$

$$x_{1,2} \leq 1$$

Schematic representation of the amplitude in MRK



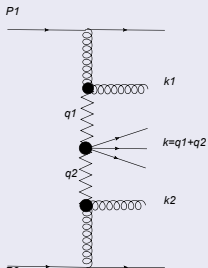
$$0 \ll q_{T1} \sim q_{T2} \sim q_{T3} \sim q_{T4} \ll \sqrt{S}$$

$$0 \ll |q_1^2| \sim |q_2^2| \sim |q_3^2| \sim |q_4^2| \ll S$$

$$y_A \gg y_1 \gg y_2 \gg y_3 \gg y_B$$

Parton Reggeization Approach

Schematic representation of the amplitude in PRA



$$0 \ll k_{T1,2} \sim q_{T1,2} \ll \sqrt{S}$$

$$0 \ll |q_1^2| \sim |q_2^2| \sim |q_3^2| \sim |q_4^2| \ll S$$

$$x_{1,2} \ll 1$$

$$q_{1,2}^\mu = x_{1,2} P_{1,2}^\mu + q_{T1,2}^\mu$$

Parton Reggeization Approach smoothly interpolates between CPM and QMRK limit of QCD

Parton Reggeization Approach (PRA)

High-energy Factorization + unintegrated PDFs + off-mass-shell Reggeized amplitudes

- A. V. Karpishkov, M. A. Nefedov and V. A. Saleev, $B\bar{B}$ angular correlations at the LHC in parton Reggeization approach merged with higher-order matrix elements, Phys. Rev. D **96** (2017) no.9, 096019.
- M. A. Nefedov, V. A. Saleev and A. V. Shipilova, Dijet azimuthal decorrelations at the LHC in the parton Reggeization approach, Phys. Rev. D **87** (2013) no.9, 094030.

Parton Reggeization Approach

Factorization formula in the PRA

$$d\sigma = \int_0^1 \frac{dx_1}{x_1} \int \frac{d^2\mathbf{q}_{T1}}{\pi} \Phi_g(x_1, t_1, \mu^2) \int_0^1 \frac{dx_2}{x_2} \int \frac{d^2\mathbf{q}_{T2}}{\pi} \Phi_g(x_2, t_2, \mu^2) \cdot d\hat{\sigma}_{\text{PRA}},$$

where $x_1 = q_1^+ / P_1^+$, $x_2 = q_2^- / P_2^-$, $\Phi(x, t, \mu^2)$ – **unintegrated PDFs**, the partonic cross-section in PRA is:

$$d\hat{\sigma}_{\text{PRA}} = \frac{|\mathcal{A}_{\text{PRA}}|^2}{2Sx_1x_2} \cdot (2\pi)^4 \delta \left(\frac{1}{2} (q_1^+ n_- + q_2^- n_+) + q_{T1} + q_{T2} - P_A \right) d\Phi_A.$$

Note the usual **flux-factor** Sx_1x_2 for **off-shell** initial-state partons.

Parton Reggeization Approach

LO unintegrated KMR PDF

$$\Phi_i(x, t, \mu^2) = \frac{T_i(t, \mu^2)}{t} \times \frac{\alpha_s(t)}{2\pi} \sum_j \int_x^1 dz \theta_{ij}^{\text{cut}} P_{ij}(z) \frac{x}{z} f_j\left(\frac{x}{z}, t\right)$$

where: $\theta_{ij}^{\text{cut}} = \theta\left((1 - \Delta_{ij}^{KMR}(t, \mu^2)) - z\right)$, and the Kimber-Martin-Ryskin(KMR) cut condition [KMR, 2001]:

$$\Delta_{ij}^{KMR}(t, \mu^2) = \frac{\sqrt{t}}{\sqrt{\mu^2} + \sqrt{t}} \delta_{ij},$$

follows from the **rapidity ordering** between the last gluon emission and the hard subprocess.

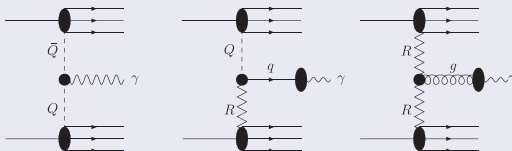
⇒ **LO normalization condition for $x \ll 1$:**

$$\int_0^{\mu^2} dt \Phi_i^{KMR}(x, t, \mu^2) \approx x f_i(x, \mu^2)$$

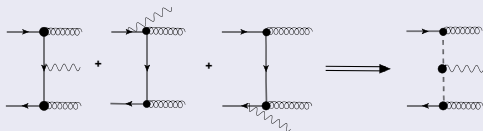
Isolated single-photon production in the PRA

V. A. Saleev. *Deep inelastic scattering and prompt photon production within the framework of the quark Reggeization hypothesis*, PHYSICAL REVIEW D 78, 034033 (2008)

B.A. Kniehl, V.A. Saleev, A.V. Shipilova, E.V. Yatsenko, *Single jet and prompt-photon inclusive production with multi-Regge kinematics: From Tevatron to LHC*, PHYSICAL REVIEW D 84, 074017 (2011)



Gauge-invariant TMD factorization in the Parton Reggeization Approach



Fadin-Sherman effective vertex [Pisma Zh.Eksp.Teor.Fiz. 23 (1976) 599-602]:

$$\Gamma_\mu(q_1, q_2) = \gamma_\mu - \hat{q}_1 \frac{n_\mu^-}{q_2} - \hat{q}_2 \frac{n_\mu^+}{q_1}, \quad q^\mu \Gamma_\mu(q_1, q_2) = 0$$

$$n_\mu^+ = 2P_2^\mu / \sqrt{S}, \quad n_\nu^- = 2P_1^\nu / \sqrt{S}, \quad \forall k : k^\pm = k^\mu n_\mu^\pm$$

Isolated photon production at Tevatron (Run I and Run II)

Run I - $\sqrt{S} = 1.8$ TeV, Run II - $\sqrt{S} = 1.96$ TeV

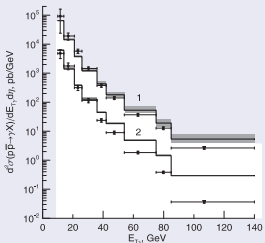


FIG. 9. The transverse-energy distributions of single prompt-photon inclusive hadroproduction measured in the pseudorapidity intervals (1) $1 < |\eta| < 2.5$ and (2) $0.9 < |\eta| < 10$ by the D0 Collaboration in Tevatron run I [15] are compared with our LO MRK predictions. The shaded bands indicate the theoretical uncertainties.

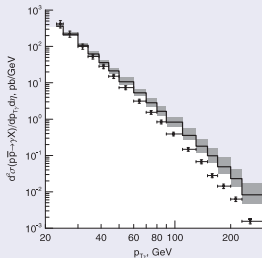


FIG. 10. The transverse-momentum distribution of single prompt-photon inclusive hadroproduction measured in the pseudorapidity interval $|\eta| < 0.9$ by the D0 Collaboration in Tevatron run II [16] is compared with our LO MRK prediction. The shaded band indicates the theoretical uncertainty.

Prompt photon plus jet associated production in the PRA

B.A. Kniehl, M.A. Nefedov, V. A. Saleev. *Prompt-photon plus jet associated photoproduction at HERA in the parton Reggeization approach*, PHYSICAL REVIEW D 89, 114016 (2014)

$$Q(q_1) + \gamma(q_2) \rightarrow q(q_3) + \gamma(q_4),$$

$$R(q_1) + \gamma(q_2) \rightarrow g(q_3) + \gamma(q_4),$$

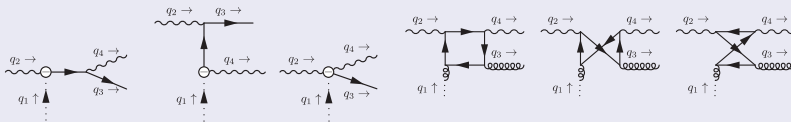
$$R(q_1) + q[\gamma](\tilde{q}_2) \rightarrow q(q_3) + \gamma(q_4),$$

$$Q(q_1) + \bar{q}[\gamma](\tilde{q}_2) \rightarrow g(q_3) + \gamma(q_4),$$

$$Q(q_1) + g[\gamma](\tilde{q}_2) \rightarrow q(q_3) + \gamma(q_4),$$

Prompt photon plus jet associated production in the PRA

Reggeized amplitudes of Lipatov's Effective Theory, $\gamma + Q \rightarrow \gamma + q$ and $\gamma + R \rightarrow \gamma + g$ (quark-box)



$$\gamma + \gamma \rightarrow \gamma + \gamma$$

V. Costantini, B. De Tollis, and G. Pistoni, *Nonlinear effects in quantum electrodynamics*, Nuovo Cimento Soc. Ital. Fis. 2A, 733 (1971).

Prompt-photon plus jet associated photoproduction at HERA

Photon transverse-energy spectra

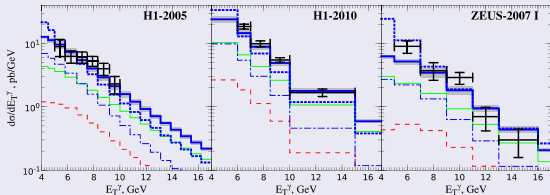


FIG. 6 (color online). E_T^γ distributions of $pe \rightarrow \gamma + j + X$ under H1-2005 [1] (left panel), H1-2010 [2] (central panel), and ZEUS-2007 I [4] (right panel) kinematic conditions. The experimental data are compared with LO PRA (boldfaced solid blue lines) and LO CPM (boldfaced dotted blue lines) predictions. The theoretical errors in the LO PRA predictions due to the freedom in the choice of ξ are indicated by the grey bands. The LO PRA predictions are decomposed into the contributions due to the partonic subprocesses in Eqs. (4) (solid green lines), (5) (dashed red lines), and (6) (dot-dashed blue lines).

Prompt-photon plus jet associated photoproduction at HERA

Photon rapidity spectra

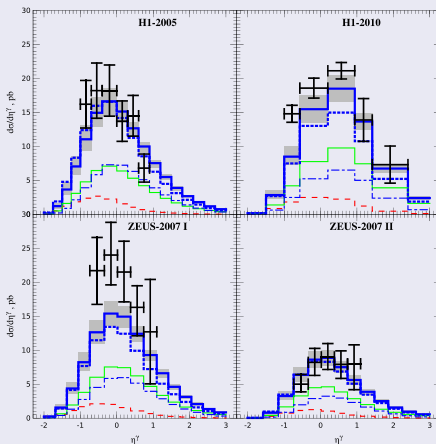


FIG. 7 (color online). η^γ distributions of $pe \rightarrow \gamma + j + X$ under H1-2005 [1] (upper left panel), H1-2010 [2] (upper right panel), ZEUS-2007 I [4] (lower left panel), and ZEUS-2007 II [4] (lower right panel) kinematic conditions. Same notation as in Fig. 6.

Prompt-photon plus jet associated photoproduction at HERA

Azimuthal angle difference spectra

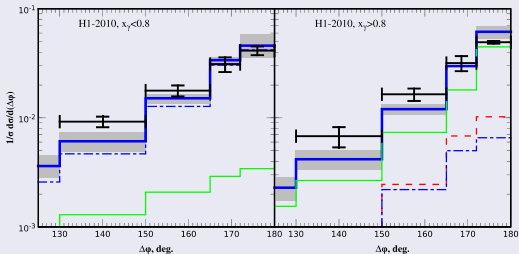
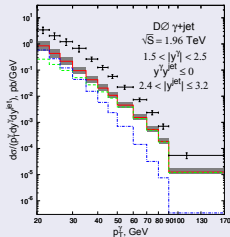
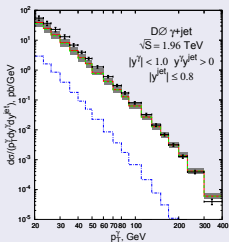


FIG. 14 (color online). Normalized $\Delta\phi$ distributions of $pe \rightarrow \gamma + j + X$ under H1-2010 [2] kinematic conditions for $x_T^{\text{LO}} < 0.8$ (left panel) and $x_T^{\text{LO}} > 0.8$ (right panel). Same notation as in the Fig. 6.

Photon plus jet associated production at TEvatron

CDF data at $\sqrt{S} = 1.96$ TeV, PHYSICAL REVIEW D 88, 072008 (2013)



Diphoton production in the PRA

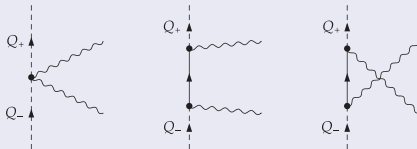
M.A. Nefedov, V. A. Saleev. *Diphoton production at the Tevatron and the LHC in the NLO approximation of the parton Reggeization approach*, PHYSICAL REVIEW D 92, 094033 (2015)

LO: $Q + \bar{Q} \rightarrow \gamma + \gamma$

NLO: $Q + R \rightarrow \gamma + \gamma + q$, $Q + \bar{Q} \rightarrow \gamma + \gamma + g$

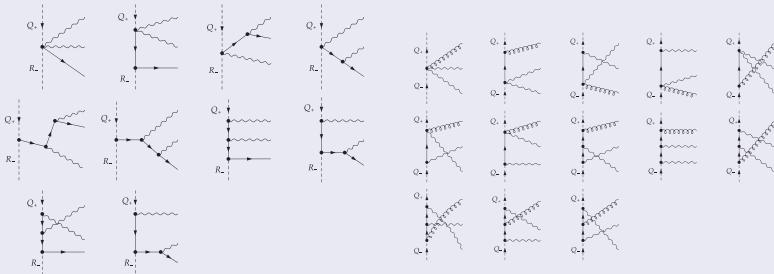
NNLO (quark-box): $R + R \rightarrow \gamma + \gamma$

LO diagrams



Diphoton production in the PRA

NLO diagrams: $Q + R \rightarrow \gamma + \gamma + q$, and $Q + \bar{Q} \rightarrow \gamma + \gamma + g$. We use original model-file ReggeQCD for FeynArts to explore Feynman rules of Lipatov EFT.



Diphoton production in the PRA

NLO* (real, $2 \rightarrow 3$) and NNLO (box-diagram) contributions

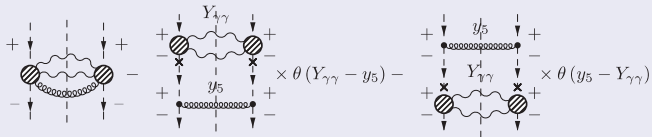
- Box-diagram contribution of $R + R \rightarrow \gamma + \gamma$ is finite, it is about 8 %.
- Contributions from $2 \rightarrow 3$ subprocesses with two photons and jets in the final state are calculated by infrared-safe way, using the smooth-cone isolation condition [S. Frixione, Physics Letters B 429 (1998) 369-374]:

$$E_T^{(had)}(r) < E_T^{(ISO)} \Gamma(r), \text{ where } \Gamma(r) = ((1 - \cos(r))/(1 - \cos(R)))^n \text{ with } n \geq 2 \text{ and } r = \sqrt{(y_5 - y_\gamma)^2 + (\phi_5 - \phi_\gamma)^2}.$$

- Subtraction term should interpolate smoothly between the strict MRK limit, when an additional parton goes deeply forward or backward in rapidity with fixed transverse momentum. Such a subtraction term is constructed in close analogy with the high-energy jets approach [J. R. Andersen, V. Del Duca, and C. D. White, J. High Energy Phys. 02 (2009) 015]

Diphoton production in the PRA

Subtraction procedure in NLO* calculations



Diphoton production in the PRA

CDF data: $\sqrt{S} = 1.96$ GeV, $q_{T\gamma} \geq 15, 17$ GeV, $|y_\gamma| \leq 1$, $R = 0.4$, $E_T^{(ISO)} = 2$ GeV.

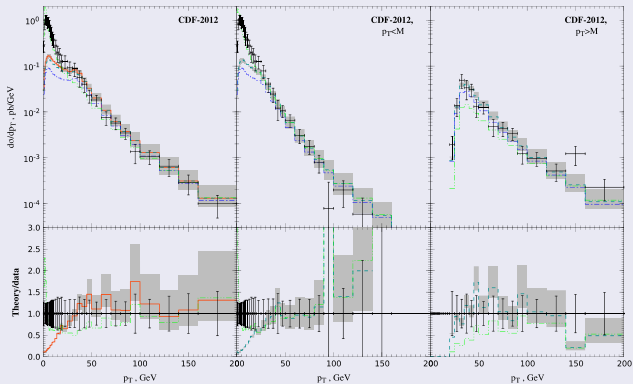
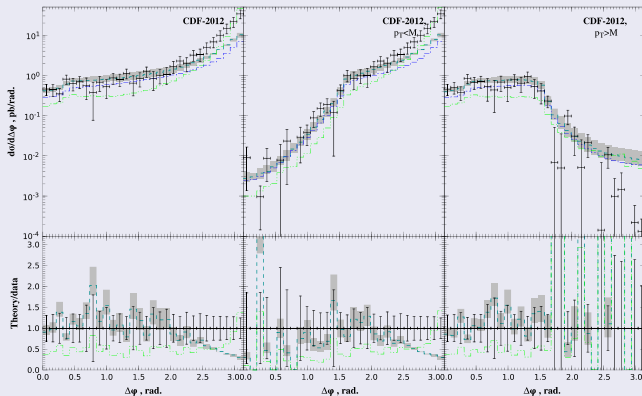


FIG. 8 (color online). The p_T spectra for the CDF-2012 data set. The thick solid curve is the sum of the contributions (5), (7) with mMRK subtraction and (17). The thick dashed curve is the sum of the first two. The thin dash-dotted curve is the contribution of the subprocess (5) only. The thin dash-double-dotted curve is the corresponding DIPHOX (NLO CPM) prediction, taken from Ref. [3]; see the text for details.

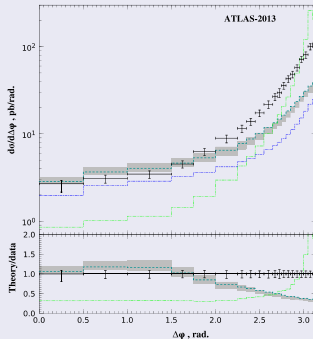
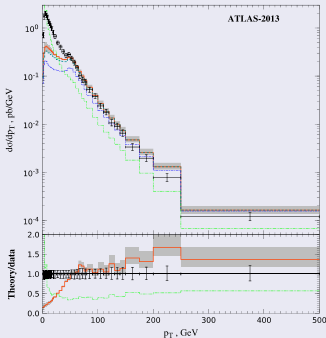
Diphoton production in the PRA

CDF data: $\sqrt{S} = 1.96$ TeV, $q_{T\gamma} \geq 15, 17$ GeV, $|y_\gamma| \leq 1$, $R = 0.4$, $E_T^{(ISO)} = 2$ GeV.



Diphoton production in the PRA

ATLAS data: $\sqrt{S} = 7$ TeV, $q_{T\gamma} \geq 22, 25$ GeV, $|y_\gamma| \leq 1.37$ and $1.52 \leq |y_\gamma| \leq 2.37$,
 $R = 0.4$, $E_T^{(ISO)} = 4$ GeV.



Prompt photon production at low energy and "small" $p_T \ll \sqrt{S}$

It is unclear how to use Collins-Soper-Sterman TMD PM for single prompt photon production

$$q_T \ll \mu, \quad \mu = Q, \text{ or } \mu = m_{J/\psi}$$

Naive TMD PM

$$d\sigma(pp \rightarrow \gamma X) = \sum_{ijk} \int dx_1 \int d^2q_{1T} \int dx_2 \int d^2q_{2T} F_i^{(p)}(x_1, \mathbf{q}_{1T}, \mu^2) \times \\ \times F_j^{(p)}(x_2, \mathbf{q}_{2T}, \mu^2) \times d\hat{\sigma}(ij \rightarrow \gamma k)$$

$$F(x, \mathbf{q}_T, \mu^2) = G(q_T) \times f(x, \mu^2)$$

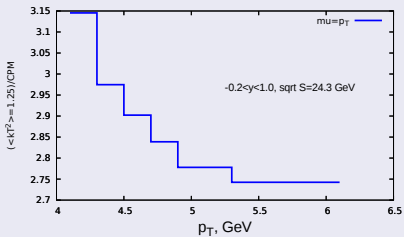
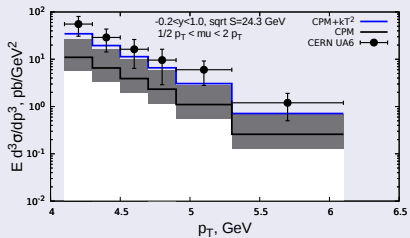
$$\int d^2q_T G(\mathbf{q}_T) = 1, \quad G(\mathbf{q}_T) = 1/(\pi b^2) \exp(-q_T^2/b^2) \text{ and } b^2 = \langle q_T^2 \rangle \simeq 1 \text{ GeV}^2.$$

Initial partons should be put on mass-shell $q_1^2 = q_2^2 = 0$

$$q_1 = x_1 P_1 + y_1 P_2 + q_{T1} = \left(x_1 \frac{\sqrt{S}}{2} + \frac{q_{T1}^2}{2x_1\sqrt{S}}, \mathbf{q}_{T1}, x_1 \frac{\sqrt{S}}{2} - \frac{q_{T1}^2}{2x_1\sqrt{S}} \right)$$

$$q_2 = x_2 P_2 + y_2 P_1 + q_{T2} = \left(x_2 \frac{\sqrt{S}}{2} + \frac{q_{T2}^2}{2x_2\sqrt{S}}, \mathbf{q}_{T2}, -x_2 \frac{\sqrt{S}}{2} + \frac{q_{T2}^2}{2x_2\sqrt{S}} \right)$$

Naive TMD PM



KMR unPDFs ($x \ll 1$) and modified NKMR unPDFs ($x < 1$)

Original KMR, unPDF $x \ll 1$

$$\int_0^{\mu^2} \Phi_i(x, t, \mu^2) dt \approx x f_i(x, t)$$

$$\Phi_i(x, t, \mu^2) \approx \frac{\partial}{\partial t} [T_i(t, \mu^2) \times x f_i(x, t)]$$

$$\begin{aligned} \Phi_i(x, t, \mu^2) &= \frac{T_i(t, \mu^2)}{t} \frac{\alpha_s(t)}{2\pi} \times \\ &\times \sum_j \int_x^1 dz P_{ij}(z) \frac{x}{z} f_i\left(\frac{x}{z}, t\right) \theta_{ij}^{cut}(z, t, \mu^2) \end{aligned}$$

$$\theta_{ij}^{cut}(z, t, \mu^2) = \theta(1 - \Delta_{ij}^{KMR}(t, \mu^2) - z)$$

$$\Delta_{ij}^{KMR}(t, \mu^2) = \frac{\sqrt{t}}{\sqrt{t} + \mu} \delta_{ij}$$

Normalized KMR unPDF, $x < 1$

$$\int_0^{\mu^2} \Phi_i(x, t, \mu^2) dt = x f_i(x, t)$$

$$\Phi_i(x, t, \mu^2) = \frac{\partial}{\partial t} [T_i(t, \mu^2, \mathbf{x}) \times x f_i(x, t)]$$

$$\begin{aligned} \Phi_i(x, t, \mu^2) &= \frac{T_i(t, \mu^2, \mathbf{x})}{t} \frac{\alpha_s(t)}{2\pi} \times \\ &\times \sum_j \int_x^1 dz P_{ij}(z) \frac{x}{z} f_i\left(\frac{x}{z}, t\right) \theta_{ij}^{cut}(z, t, \mu^2) \end{aligned}$$

$$\theta_{ij}^{cut}(z, t, \mu^2) = \theta(1 - \Delta_{ij}(t, \mu^2) - z)$$

$$\Delta_{ij}(t, \mu^2) = \frac{\sqrt{t}}{\sqrt{t} + \mu}$$

KMR unPDFs ($x \ll 1$) and modified NKMR unPDFs ($x < 1$)Exact Sudakov FF $T_i(t, \mu^2, x)$

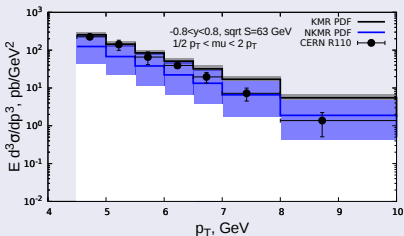
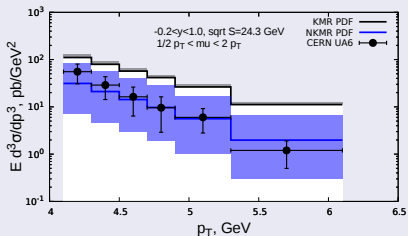
$$T_i(t, \mu^2, x) = \exp \left[- \int_t^{\mu^2} \frac{dt'}{t'} \frac{\alpha_s(t')}{2\pi} (\tau_i(t', \mu^2) + \delta\tau_i(t, x, \mu^2)) \right]$$

$$\tau_i(t', \mu^2) = \sum_j \int_0^1 dz \theta_{ij}^{cut}(z, t', \mu^2) z P_{ij}(z)$$

$$\delta\tau_i(t', x, \mu^2) = \sum_j \int_0^1 (1 - \theta_{ij}^{cut}(z, t', \mu^2)) \times \\ \times \left[z P_{ji}(z) - \frac{x}{z} \frac{f_j(\frac{x}{z}, t')}{x f_i(x, t')} P_{ij}(z) \theta(z - x) \right]$$

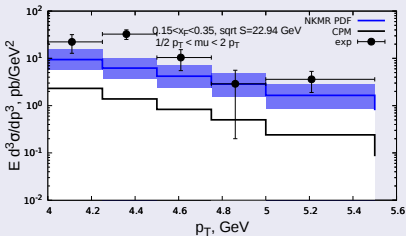
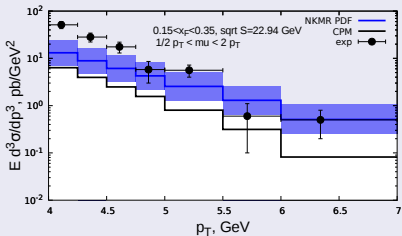
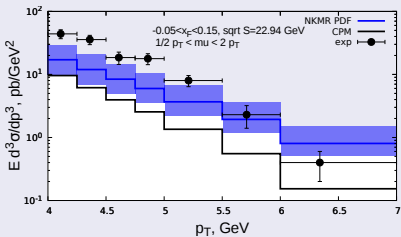
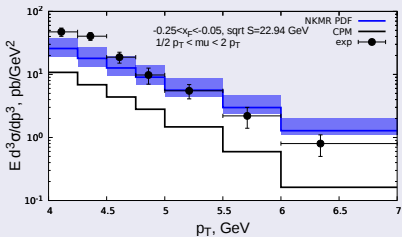
Prompt photon production (pp , UA6 and R110) in the PRA at low energy

KMR PDFs versus NKMR PDFs



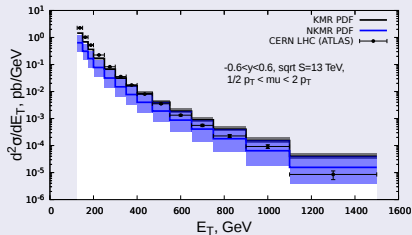
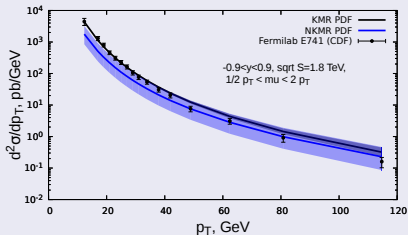
Prompt photon production (πp , WA70) in the PRA at low energy

KMR PDFs versus NKMR PDFs



Prompt photon production in the PRA at high energy

KMR PDFs versus NKMR PDFs

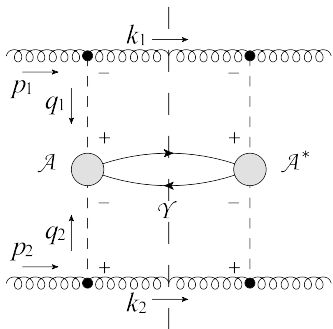


CONCLUSIONS

- We suggest Parton Reggeization Approach which smoothly interpolates between Collinear Factorization and High-Energy Factorization. Treating of initial partons as Reggeized partons of Lipatov's EFT guarantees Gauge Invariance of hard scattering amplitudes.
- We suggest modified KMR unPDFs, NKMR PDFs, which can be used at arbitrary $x < 1$.
- We demonstrate opportunity of the NLO calculations in the PRA: M.N., V.S. *From LO to NLO in the parton Reggeization approach*, EPJ Web Conf. 191 (2018) 04007; M.N., V.S. *On the one-loop calculations with Reggeized quarks*, Mod.Phys.Lett. A32 (2017) no.40, 1750207; M.N. *One-loop corrections to multiscale effective vertices in the EFT for Multi-Regge processes in QCD*, PoS DIS2019 (2019) 064; M.N. *Computing one-loop corrections to effective vertices with two scales in the EFT for Multi-Regge processes in QCD*, Nucl.Phys. B946 (2019) 114715.
- We find importance of power corrections, off-shell effects and gauge invariance in large- p_T region ($p_T \sim \mu$) for production of prompt photons, DY pairs (see Maxim Nefedov talk) and charmonia (see Igor Denisenko talk).

Thank you for your attention!

LO factorization formula in the PRA



$$n^+ = (1, 0, 0, -1), \quad n^- = (1, 0, 0, +1), \quad q^\pm = (qn^\pm)$$

Auxiliary hard CPM subprocess:

$$g(p_1) + g(p_2) \rightarrow g(k_1) + \mathcal{Y}(P_A) + g(k_2),$$

where $p_1^2 = 0$, $p_1^- = 0$, $p_2^2 = 0$, $p_2^+ = 0$.

Kinematic variables ($0 < z_{1,2} < 1$):

$$z_1 = \frac{p_1^+ - k_1^+}{p_1^+}, \quad z_2 = \frac{p_2^- - k_2^-}{p_2^-},$$

Two limits where $|\overline{\mathcal{M}}|^2$ factorizes:

- Collinear limit:** $q_{T1,2}^2 \ll \mu^2$, $z_{1,2}$ - arbitrary,
- Multi-Regge limit:** $z_{1,2} \ll 1$, $q_{T1,2}^2$ - arbitrary.

LO factorization formula in the PRA

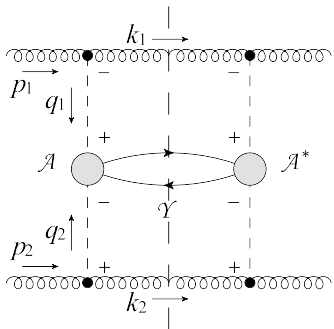
Auxiliary hard CPM subprocess:

$$g(p_1) + g(p_2) \rightarrow g(k_1) + \mathcal{Y}(P_A) + g(k_2),$$

- 1 **Collinear limit:** $q_{T1,2}^2 \ll \mu^2$, $z_{1,2}$ – arbitrary:

$$|\overline{\mathcal{M}}|^2_{\text{CL}} \simeq \frac{4g_s^4}{q_1^2 q_2^2} P_{gg}(z_1) P_{gg}(z_2) \frac{|\overline{\mathcal{A}_{CPM}}|^2}{z_1 z_2},$$

where $|\overline{\mathcal{A}_{CPM}}|^2$ – amplitude $g + g \rightarrow \mathcal{Y}$ with **on-shell** initial-state partons, $P_{gg}(z)$ – DGLAP $g \rightarrow g$ splitting function.



LO factorization formula in the PRA

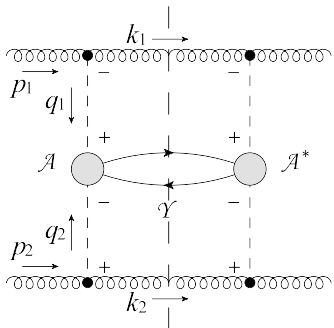
Auxiliary hard CPM subprocess:

$$g(p_1) + g(p_2) \rightarrow g(k_1) + \mathcal{Y}(P_A) + g(k_2),$$

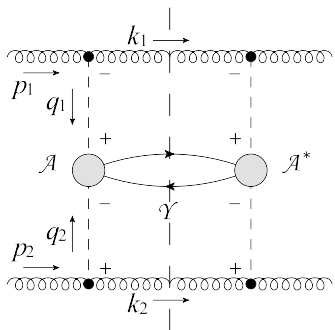
2 Multi-Regge limit: $z_{1,2} \ll 1$
 ($\Leftrightarrow \Delta y_{1,2} \gg 1$), $\mathbf{q}_{T1,2}^2$ - arbitrary:

$$|\overline{\mathcal{M}}|^2_{\text{MRK}} \simeq \frac{4g_s^4}{\mathbf{q}_{T1}^2 \mathbf{q}_{T2}^2} \tilde{P}_{gg}(z_1) \tilde{P}_{gg}(z_2) \frac{|\overline{\mathcal{A}_{PRA}}|^2}{z_1 z_2},$$

where $\tilde{P}_{gg}(z) = 2C_A/z$ and $|\overline{\mathcal{A}_{PRA}}|^2$ is the **gauge-invariant** amplitude
 $R_+(q_1) + R_-(q_2) \rightarrow \mathcal{Y}$ with **Reggeized**
 (**off-shell**) partons in the initial state.



LO factorization formula in the PRA



Auxiliary hard CPM subprocess:

$$g(p_1) + g(p_2) \rightarrow g(k_1) + \mathcal{Y}(P_A) + g(k_2),$$

Modified MRK approximation: $z_{1,2}$ and $\mathbf{q}_{T1,2}^2$ - arbitrary:

$$|\overline{\mathcal{M}}|^2_{\text{mMRK}} \simeq \frac{4g_s^4}{q_1^2 q_2^2} P_{gg}(z_1) P_{gg}(z_2) \frac{|\overline{\mathcal{A}_{PRA}}|^2}{z_1 z_2},$$

where $q_{1,2}^2 = \mathbf{q}_{T1,2}^2 / (1 - z_{1,2})$, has correct **collinear** and **Multi-Regge** limits!

Factorization formula in the PRA

Substituting the $|\overline{\mathcal{M}}|^2_{\text{mMRK}}$ to the factorization formula of CPM and changing the variables we get:

$$d\sigma = \int_0^1 \frac{dx_1}{x_1} \int \frac{d^2\mathbf{q}_{T1}}{\pi} \tilde{\Phi}_g(x_1, t_1, \mu^2) \int_0^1 \frac{dx_2}{x_2} \int \frac{d^2\mathbf{q}_{T2}}{\pi} \tilde{\Phi}_g(x_2, t_2, \mu^2) \cdot d\hat{\sigma}_{\text{PRA}},$$

where $x_1 = q_1^+/P_1^+$, $x_2 = q_2^-/P_2^-$, $\tilde{\Phi}(x, t, \mu^2)$ – “tree-level” **unintegrated PDFs**, the partonic cross-section in PRA is:

$$d\hat{\sigma}_{\text{PRA}} = \frac{|\overline{\mathcal{A}}_{\text{PRA}}|^2}{2Sx_1x_2} \cdot (2\pi)^4 \delta \left(\frac{1}{2} \left(q_1^+ n_- + q_2^- n_+ \right) + q_{T1} + q_{T2} - P_A \right) d\Phi_A.$$

Note the usual **flux-factor** Sx_1x_2 for **off-shell** initial-state partons.

LO unintegrated PDF

The “tree-level” unPDF:

$$\tilde{\Phi}_g(x, t, \mu^2) = \frac{1}{t} \frac{\alpha_s}{2\pi} \int_x^1 dz P_{gg}(z) \cdot \frac{x}{z} f_g\left(\frac{x}{z}, \mu^2\right).$$

contains collinear divergence at $t \rightarrow 0$ and IR divergence at $z \rightarrow 1$.

In the “dressed” unPDF collinear divergence is regulated by **Sudakov formfactor** $T(t, \mu^2)$:

$$\Phi_i(x, t, \mu^2) = \frac{T_i(t, \mu^2)}{t} \times \frac{\alpha_s(t)}{2\pi} \sum_j \int_x^1 dz \theta_{ij}^{\text{cut}} P_{ij}(z) \frac{x}{z} f_j\left(\frac{x}{z}, t\right)$$

where: $\theta_{ij}^{\text{cut}} = \theta\left((1 - \Delta_{ij}^{KMR}(t, \mu^2)) - z\right)$, and the Kimber-Martin-Ryskin(KMR) **cut condition** [KMR, 2001]:

$$\Delta_{ij}^{KMR}(t, \mu^2) = \frac{\sqrt{t}}{\sqrt{\mu^2} + \sqrt{t}} \delta_{ij},$$

follows from the **rapidity ordering** between the last gluon emission and the hard subprocess.

Factorization formula in the PRA

LO unintegrated KMR PDF

$$\Phi_i^{KMR}(x, t, \mu^2) = \frac{T_i(t, \mu^2)}{t} \times \frac{\alpha_s(t)}{2\pi} \sum_j \int_x^1 dz \theta_{ij}^{\text{cut}} P_{ij}(z) \frac{x}{z} f_j\left(\frac{x}{z}, t\right)$$

\Rightarrow LO normalization condition for $x \ll 1$:

$$\int_0^{\mu^2} dt \Phi_i^{KMR}(x, t, \mu^2) \approx x f_i(x, \mu^2)$$